

THERMODYNAMIC STABILITY AND FORMATION MECHANISM OF IRON(III) COMPLEX WITH *N*-PYRIDOXYL-*o*- HYDROXYANILINE: ROLE OF PHENOLATE OXYGEN ON THE ENHANCEMENT OF THE STABILITY

TOMOHIRO OZAWA, KOICHIRO JITSUKAWA, HIDEKI MASUDA and
HISAHIKO EINAGA*

Department of Applied Chemistry, Faculty of Engineering, Nagoya Institute of Tech-
nology, Gokiso-cho, Showa-ku, Nagoya 466, Japan

(Received 2 February 1994; accepted 20 October 1994)

Abstract—A new terdentate ligand, *N*-pyridoxyl-*o*-hydroxyaniline (**1**, H₂pha), was synthesized and the formation of its iron(III) complex was thermodynamically and kinetically investigated (0.10 mol dm⁻³ NaClO₄; 25°C). The ligand forms a very stable bis(ligand)iron(III) complex ($\log \beta_{12} = 45.8 \pm 0.2$; β_{12} (mol⁻² dm⁶) = [Fe(Hpha)₂]⁺/[Fe³⁺][Hpha⁻]²) in comparison with other *N*^z-pyridoxyl-L-amino acid-type terdentate ligands with benzyl (**2**), methyl (**3**), and indolylmethyl (**4**) groups, indicating that an intramolecular interaction as well as a high affinity of phenolato oxygen to the central metal atom greatly contributes to the stability of the bis(ligand)iron(III) complex of **1**. The rate constants for the iron(III) complex of **1** are $(1.40 \pm 0.20) \times 10^2$ mol⁻¹ dm³ s⁻¹ for the two parallel pathways of Fe³⁺ + H₃pha⁺ (k_{33}) and FeOH²⁺ + H₄pha²⁺ (k_{24}) ($k_{33} + k_{24}K_{OH}^{11}K_{a(amNH)}$, where K_{OH}^{11} and $K_{a(amNH)}$ are the hydrolysis constant of iron(III) and protonation constant of **1** at the amino nitrogen) and $(2.44 \pm 0.30) \times 10^2$ mol⁻¹ dm³ s⁻¹ for the pathway of FeOH²⁺ + H₃pha⁺ (k_{23}). The comparison of these rate constants with those of the iron(III) complexes of **2**, **3**, and **4** suggests that the complex formation mechanism is given by the rate-determining coordination of the phenolato oxygen of pyridoxyl moiety to iron(III), followed by the rapid donations of other ligating groups.

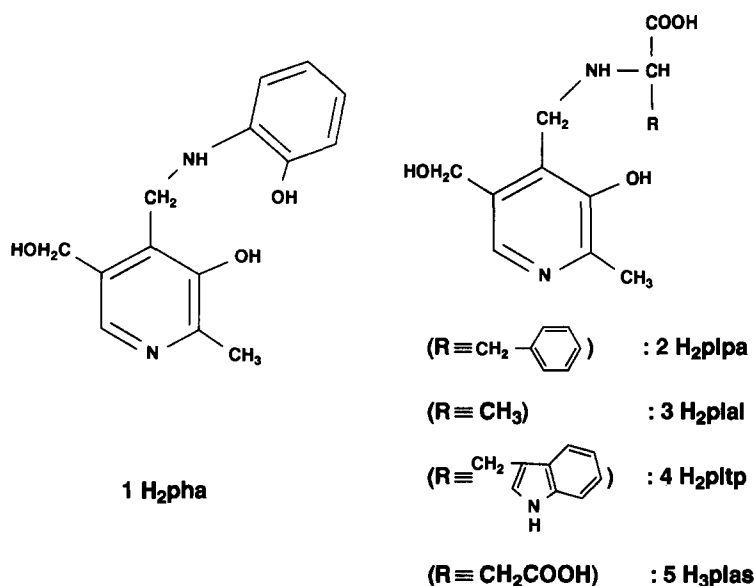
The design and synthesis of an artificial siderophore is our recent concern.^{1,2} It has been found^{1,2} that terdentate *N*^z-pyridoxyl-L-amino acid-type ligands (*N*^z-pyridoxyl-L-phenylalanine (**2**, H₂plpa), *N*^z-pyridoxyl-L-alanine (**3**, H₂plal), and *N*^z-pyridoxyl-L-tryptophan (**4**, H₂pltp)) and a tetradentate one *N*^z-pyridoxyl-L-aspartic acid (**5**, H₃plas) form thermodynamically stable iron(III) complexes, especially for the bis(ligand)iron(III) complex of **5** ($\log \beta_{12} = 48.33 \pm 0.21$; β_{12} (mol⁻² dm⁶) = [Fe(Hplas)₂]⁻/[Fe³⁺][Hplas²⁻]²).¹

Apart from these facts, Enterobactin (H₃ent), a natural siderophore with three catechol units,

has been known to have an exceptionally large stability constant ($\log \beta_{11} = 49$;³ β_{11} (mol⁻¹ dm³) = [Fe(ent)]/[Fe³⁺][ent³⁻]). Thus, designing the ligands to those containing catecholate, or more simply phenolate groups would be desirable in order to increase the stability of their iron(III) complexes. Accordingly, the synthesis of a new ligand containing two phenolate oxygens in this pyridoxal-type chelator is important in order to compare the role of aminophenolate and aminocarboxylate moieties on the stability of the iron(III) complexes.

This paper is concerned with the stability and the formation reaction mechanism of the iron(III) complex with *N*-pyridoxyl-*o*-hydroxyaniline (**1**, H₂pha), a new ligand containing two phenolate ligating groups, as an analogue of *N*^z-pyridoxyl-L-amino acids.

* Author to whom correspondence should be addressed.



EXPERIMENTAL

Materials

The ligand **1** was prepared by the same procedure in a previous paper¹ with some modifications. This ligand was characterized by the ¹H NMR method. Found: C, 52.4; H, 5.5; N, 8.7%. Calc. for C₁₄H₁₆N₂O₃ · H₂O · NaCl: C, 52.6; H, 5.4; N, 8.8%.

An iron(III) solution was prepared as described elsewhere.² All materials except the ligand were supplied from Wako Pure Chemicals Ind., Ltd., Osaka, and used without further purification.

Measurements

The protonation constants of **1** were determined spectrophotometrically at the wavelengths specific to its respective protonation equilibria as will be described later. The thermodynamic stability constants of iron(III) complex of **1** were also determined spectrophotometrically by recording the absorbance change with equilibrium acidity at the wavelengths of 600 nm for the mono(ligand) iron(III) complex and 525 nm for the bis(ligand) iron(III) complex, respectively. Electronic absorption spectra were recorded on JASCO spectrophotometers, models UVIDEc-660 and Ubest-35.

Complex formation kinetics were followed by means of a stopped-flow spectrophotometric method under the pseudo-first-order reaction conditions of $C_L \gg C_M$, where C_M and C_L represent the total concentrations of iron(III) and the ligand, respectively. The apparatus and general procedures have been described elsewhere.⁴

The ionic strength of the solution was kept constant at 0.10 mol dm⁻³ sodium perchlorate; the buffer solutions were used as described in a previous paper.¹

The hydrogen ion concentration, [H⁺], was calculated according to eq. (1).

$$-\log [H^+] = \text{pH}_{\text{meas}} + \log f_{H^+} \quad (1)$$

Here, pH_{meas} represents the measured pH value; the activity coefficient, $\log f_{H^+}$, of -0.08^5 was adopted here.

RESULTS

Electronic absorption spectra

Absorption spectra of **1** and its iron(III) complex are depicted in Fig. 1 together with the spectrum of **3** for comparison. An intense absorption band is observed in both spectra of these two ligands at $(30.0\text{--}40.0) \times 10^3 \text{ cm}^{-1}$, which is assignable to the $\pi^* \leftarrow \pi$ transition of the aromatic ring chromophore. The free ligand **1** has an additional broad absorption band below $30.0 \times 10^3 \text{ cm}^{-1}$, as compared with that of **3**, being due to the $\pi^* \leftarrow \pi$ transition of the aminophenol chromophore.

A new and broad absorption band with less intensity than that in the ultraviolet region appears only in the iron(III) complex at $(16.0\text{--}26.5) \times 10^3 \text{ cm}^{-1}$. This band can be assigned to a ligand-to-metal charge-transfer (CT) transition ($t_{2g}(\text{O}_h) \leftarrow \pi$).^{1,2}

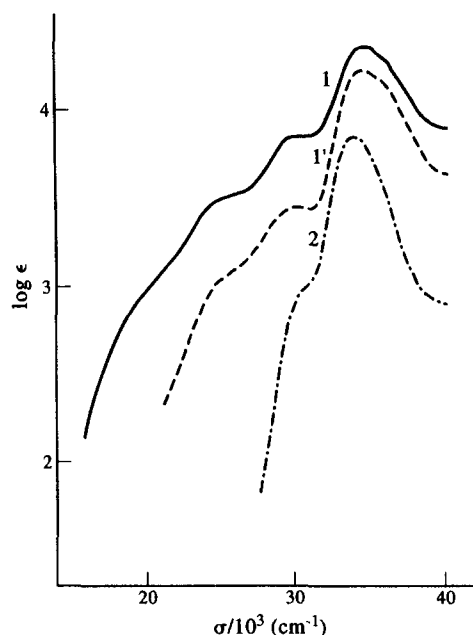


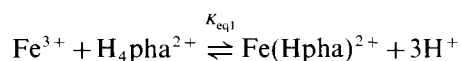
Fig. 1. Electronic absorption spectra of the ligands **1** and **3** and the iron(III) complex of **1**. **1**, $[\text{Fe}(\text{Hpha})_2]^+$ (pH 2.03); **1'**, Hpha^- (pH 9.34); **2**, Hplal^- (pH 9.09).

stants are listed in Table 1 together with those of the ligands of concern. It is interesting to point out here that the basicity of the amino nitrogen donor atom decreases markedly by its direct attachment to an aromatic ring (*cf* $K_{a(\text{amNH})}$ of **1** and **2–5**) as is expected from the protonation constants of aniline ($\log K_a = 4.65$)⁷ and dimethylamine ($\log K_a = 10.77$).⁸

Formation and stability

The ligand **1** serves potentially as a terdentate ligand and is expected to form a bis(ligand) metal(III) complex as well as a mono(ligand) metal(III) complex with iron(III) capable of taking an octahedral coordination structure.

The stability constant of the mono(ligand) iron(III) complex of **1** was determined from the experimental relation between the absorbance and $-\log[\text{H}^+]$ shown in Fig. 2. Equilibrium (I) and its constant, K_{eq1} , can be defined on the basis of the protonation constants of **1**.



$$C_{\text{M}} = [\text{Fe}^{3+}] + [\text{FeOH}^{2+}]$$

$$\beta_{11} = [\text{Fe}(\text{Hpha})^{2+}] / [\text{Fe}^{3+}][\text{Hpha}^-] (C_{\text{M}} \gg C_{\text{L}}) \quad (\text{I})$$

Here, $\text{Fe}(\text{Hpha})^{2+}$ indicates the mono(ligand) iron(III) complex with pyridyl-nitrogen-protonated form, which is practical under the experimental conditions investigated.^{1,2} In an analogous

Protonation constants

Protonation constants of **1** were determined spectrophotometrically according to the literature procedure⁶ by following the wavelengths at 300 nm for phenolate oxygen of aminophenol moiety ($K_{a(\text{apOH})}$), 330 nm for phenolate oxygen of pyridoxyl moiety ($K_{a(\text{pyOH})}$), 280 nm for pyridyl nitrogen ($K_{a(\text{pyNH})}$), and 330 nm for amino nitrogen ($K_{a(\text{amNH})}$), respectively. These protonation con-

Table 1. Protonation constants^a

Ligand	$\log K_{a(\text{apOH})}$	$\log K_{a(\text{pyOH})}$	$\log K_{a(\text{pyNH})}$	$\log K_{a(\text{amNH})}$	Remarks	Ref.	
1 (H_2pha) ^b	10.20 ± 0.02	8.31 ± 0.03	4.85 ± 0.02	2.55 ± 0.02	^c	This work	
Ligand	$\log K_{a(\text{amNH})}$	$\log K_{a(\text{pyOH})}$	$\log K_{a(\text{mcCOOH})}$	$\log K_{a(\text{pyNH})}$	$\log K_{a(\text{COOH})}$	Remarks	Ref.
2 (H_2plpa) ^f	10.23 ± 0.02	7.60 ± 0.02	—	3.08 ± 0.02	2.58 ± 0.05	^e	1
3 (H_2plal) ^c	10.34 ± 0.02	7.85 ± 0.02	—	3.21 ± 0.03	2.35 ± 0.05	^e	1
4 (H_2pltp) ^c	10.37 ± 0.04	8.45 ± 0.03	—	3.12 ± 0.03	2.38 ± 0.06	^e	2
5 (H_3plas) ^d	10.61 ± 0.03	8.17 ± 0.03	3.85 ± 0.05	3.06 ± 0.02	2.10 ± 0.05	^e	1

^a All K_a values are in $\text{mol}^{-1} \text{dm}^3$.

^b $K_{a(\text{apOH})} = [\text{HL}^-]/[\text{H}^+][\text{L}^{2-}]$, $K_{a(\text{pyOH})} = [\text{H}_2\text{L}]/[\text{H}^+][\text{HL}^-]$, $K_{a(\text{pyNH})} = [\text{H}_3\text{L}^+]/[\text{H}^+][\text{H}_2\text{L}]$, and $K_{a(\text{amNH})} = [\text{H}_4\text{L}^{2+}]/[\text{H}^+][\text{H}_3\text{L}^+]$. L denotes fully-deprotonated ligand species.

^c $K_{a(\text{amNH})} = [\text{HL}^-]/[\text{H}^+][\text{L}^{2-}]$, $K_{a(\text{pyOH})} = [\text{H}_2\text{L}]/[\text{H}^+][\text{HL}^-]$, $K_{a(\text{pyNH})} = [\text{H}_3\text{L}^+]/[\text{H}^+][\text{H}_2\text{L}]$, and $K_{a(\text{COOH})} = [\text{H}_4\text{L}^{2+}]/[\text{H}^+][\text{H}_3\text{L}^+]$.

^d $K_{a(\text{amNH})} = [\text{HL}^{2-}]/[\text{H}^+][\text{L}^{3-}]$, $K_{a(\text{pyOH})} = [\text{H}_2\text{L}^-]/[\text{H}^+][\text{HL}^{2-}]$, $K_{a(\text{mcCOOH})} = [\text{H}_3\text{L}]/[\text{H}^+][\text{H}_2\text{L}^-]$, $K_{a(\text{pyNH})} = [\text{H}_4\text{L}^+]/[\text{H}^+][\text{H}_3\text{L}]$, and $K_{a(\text{COOH})} = [\text{H}_5\text{L}^{2+}]/[\text{H}^+][\text{H}_4\text{L}^+]$.

^e 0.10 mol dm^{-3} (NaClO_4), 25°C .

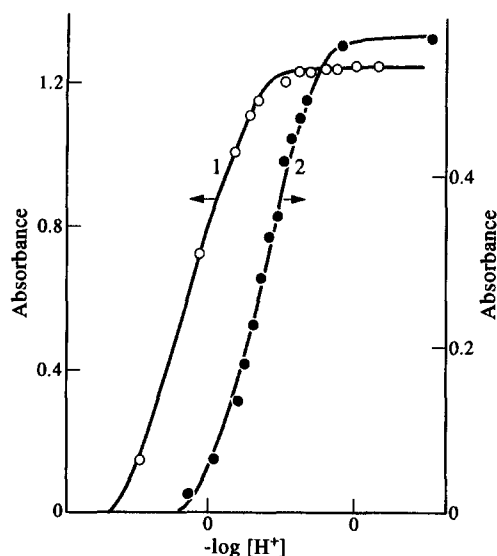


Fig. 2. Relation between absorbance and $-\log[\text{H}^+]$ for mono(ligand)iron(III) complexes of **1** and **3**. $C_M \gg C_L$. 1, iron(III)-**1** system; C_M , $2.01 \times 10^{-3} \text{ mol dm}^{-3}$; C_L , $1.00 \times 10^{-4} \text{ mol dm}^{-3}$; λ , 600 nm; 2, iron(III)-**3** system; C_M , $2.00 \times 10^{-3} \text{ mol dm}^{-3}$; C_L , $1.00 \times 10^{-4} \text{ mol dm}^{-3}$; λ , 475 nm; 0.10 mol dm^{-3} (NaClO_4), 25°C . The solid lines are theoretical ones drawn by using the protonation, stability, and hydrolysis constants given in the text and tables.

way as has been reported,^{1,2} eq. (2) can be easily derived by adopting Beer's law:

$$\log \left\{ \frac{(A_{\max}^1 - A^1)}{(A^1 - A_{\min}^1)} \right\} = \log [\text{H}^+]^3 (1 + K_{\text{OH}}^{11}/[\text{H}^+]) - \log K_{\text{eq1}} C_M \quad (2)$$

Here, A_{\max}^1 , A_{\min}^1 , and A^1 represent the absorbance of the mono(ligand)iron(III) complex, that of the free ligand, and that of the complex and the free ligand coexisting at $[\text{H}^+]$, respectively, K_{OH}^{11} is the hydrolysis constant of iron(III) $\{K_{\text{OH}}^{11} (\text{mol dm}^{-3}) = [\text{FeOH}^{2+}][\text{H}^+]/[\text{Fe}^{3+}]; \log K_{\text{OH}}^{11} = -2.78$ 0.10 mol dm^{-3} (NaClO_4), $25^\circ\text{C}\}$.⁹

Plotting the left-hand term *vs* the hydrogen ion concentration term of eq. (2) from the data in Fig. 2 (Curve 1) gave a straight line with a slope of unity, which can be represented as $Y = 1.01X + 2.41$ ($Y \equiv \log \left\{ \frac{(A_{\max}^1 - A^1)}{(A^1 - A_{\min}^1)} \right\}$, $X \equiv \log [\text{H}^+]^3 (1 + K_{\text{OH}}^{11}/[\text{H}^+])$). The value of K_{eq1} was calculated from the intercept; β_{11} was calculated from this K_{eq1} according to eq. (3)

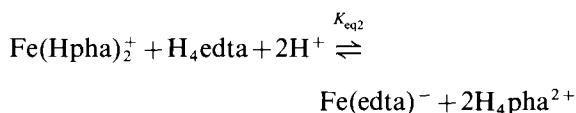
$$\beta_{11} (\text{mol}^{-1} \text{ dm}^3) = K_{\text{a}(\text{apOH})} K_{\text{a}(\text{pyOH})} K_{\text{a}(\text{amNH})} K_{\text{eq1}} \quad (3)$$

to be $\log \beta_{11} = 21.35 \pm 0.18$.

The stability constant of the bis(ligand)iron(III) complex of **1** could not be estimated in this manner

under the conditions of $C_L \gg C_M$, because **1** formed a very stable bis(ligand)iron(III) complex even in the strong acidity region below pH 1.0. Consequently, we attempted to estimate this stability constant by making competition to iron(III) of the ligand **1** with ethylenediamine-*N,N,N',N'*-tetraacetic acid (H_4edta), because the $\text{Fe}(\text{edta})^-$ complex has high stability constant (*vide infra*) and has negligibly small absorbance as well as the free $\text{H}_n\text{edta}^{(n-4)+}$, **1**, and aqua-iron(III) ion as compared with the bis(ligand)iron(III) complex at the specified wavelength of 525 nm.

For the bis(ligand)iron(III) complex of **1**, Equilibrium (II)



$$\beta_{12} = [\text{Fe}(\text{Hpha})_2^+]/[\text{Fe}^{3+}][\text{Hpha}^-]^2,$$

$$\beta_{\text{Fe}(\text{edta})^-} = [\text{Fe}(\text{edta})^-]/[\text{Fe}^{3+}][\text{edta}^{4-}] \quad (\text{II})$$

can be defined in an acidic aqueous solution of pH 1.50, where the competing ligand is expected to be present mainly in the form of tetra-protonated species ($\log K_{\text{a1}} = 10.26$, $\log K_{\text{a2}} = 6.16$, $\log K_{\text{a3}} = 2.67$, and $\log K_{\text{a4}} = 2.00$).¹⁰ On the basis of materials balance and the conditions of $C_L \gg C_M$, the equilibrium constant, K_{eq2} , can be represented by eq. (4),

$$C_{\text{edta}} - \{(A_{\max}^2 - A^2)/A_{\max}^2\} C_M = \{C_L^2/(K_{\text{eq2}}[\text{H}^+]^2)\} (A_{\max}^2 - A^2)/A^2 \quad (4)$$

where C_{edta} denotes the total concentration of ethylenediamine-*N,N,N',N'*-tetraacetic acid, and A_{\max}^2 and A^2 represent the absorbances of $\text{Fe}(\text{Hpha})_2^+$ and the mixture of $\text{Fe}(\text{Hpha})_2^+$ and $\text{Fe}(\text{edta})^-$ whose fraction is determined by C_{edta} , respectively.

Plotting the relation between $C_{\text{edta}} - \{(A_{\max}^2 - A^2)/A_{\max}^2\} C_M$ and $(A_{\max}^2 - A^2)/A^2$ gave a straight line passing through the origin represented as $Y = (2.09 \times 10^{-4})X$, from the slope of which K_{eq2} was obtained. The stability constant, β_{12} , was calculated from this K_{eq2} by the use of eq. (5).

$$\beta_{12} = \beta_{\text{Fe}(\text{edta})^-} (K_{\text{a}(\text{apOH})} K_{\text{a}(\text{pyOH})} K_{\text{a}(\text{amNH})})^2 / K_{\text{a1}} K_{\text{a2}} K_{\text{a3}} K_{\text{a4}} K_{\text{eq2}} \quad (5)$$

using $\log \beta_{\text{Fe}(\text{edta})^-} = 25.1$.¹⁰ The value of β_{12} thus estimated is listed in Table 2.

Kinetics and mechanism

The time-course of the absorbance of iron(III)-**1** system showed an exponential curve over 3.5 half-

Table 2. Stability constants^a

Complex	log β_{11}	log β_{12}	Remarks	Ref.
6 Fe(Hpha) ₂ ⁺	21.35 ± 0.18	45.8 ± 0.2	0.10 mol dm ⁻³ (NaClO ₄), 25°C	This work
7 Fe(Hplpa) ₂ ⁺ ^b	18.77 ± 0.14	39.06 ± 0.26	0.01 mol dm ⁻³ (NaClO ₄), 25°C	1
Fe(Hplal) ₂ ⁺ ^c	19.50 ± 0.13	39.81 ± 0.20	0.10 mol dm ⁻³ (NaClO ₄), 25°C	1
Fe(Hpltp) ₂ ⁺ ^d	22.54 ± 0.19	38.29 ± 0.28	0.10 mol dm ⁻³ (NaClO ₄), 25°C	2
Fe(Hplas) ₂ ⁻ ^e	21.86 ± 0.16	48.33 ± 0.21	0.10 mol dm ⁻³ (NaClO ₄), 25°C	1
Fe(Hgly) ₂ ³⁺ ^f	2.03	3.7	3.0 mol dm ⁻³ , 25°C	12
Fe(pmgly) ₂ ⁺ ^g	16.09	23	0.1 mol dm ⁻³ , 25°C	13
Fe(ida) ₂ ⁻ ^h	10.72	20.14	0.5 mol dm ⁻³ , 25°C	14

^a β_{11} values in mol⁻¹ dm³; β_{12} values in mol⁻² dm⁶.

^b Iron(III) complex of 2.

^c Iron(III) complex of 3.

^d Iron(III) complex of 4.

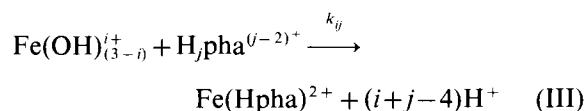
^e Iron(III) complex of 5.

^f Hgly; glycine.

^g Hpmgly; *N*-(phosphomonoethyl)glycine.

^h H₃ida; iminodiacetic acid.

life periods in the acidity region of pH 1.2–2.5 under the pseudo-first-order kinetic conditions of $C_L \gg C_M$. This fact indicates that only one measurable step is included in the complex formation kinetics. Furthermore, plotting the observed rate constant, k_{obsd} , against C_L/C_M gave a linear relation that can be extrapolated to the origin. This finding reveals that the slow coordination of the first ligand molecule of **1** to iron(III) ion to form a mono (ligand)iron(III) complex species as an intermediate exists prior to the fast coordination of the second one to form the thermodynamically more stable bis(ligand)iron(III) complex; *i.e.* the rate-limiting stage is the coordination of the first ligand to the central metal atom. Hence, the following Reaction (III)



$$\begin{aligned} d[\text{Fe}(\text{Hpha})^{2+}]/dt &= \sum_{i=2}^3 \sum_{j=3}^4 k_{ij} [\text{Fe}(\text{OH})_{3-i}^{i+}] [\text{H}_j\text{pha}^{(j-2)+}] \\ &= k_{\text{obsd}} C_M \quad (C_L \gg C_M) \end{aligned} \quad (6)$$

$$k_{\text{obsd}} = \sum_{i=2}^3 \sum_{j=3}^4 k_{ij} C_L / (1 + K_{\text{OH}}^{11} / [\text{H}^+]) \alpha_{\text{H}}$$

$$\begin{aligned} \alpha_{\text{H}} &\equiv K_{\text{a}(\text{apOH})} K_{\text{a}(\text{pyOH})} K_{\text{a}(\text{amNH})} [\text{H}^+]^3 \\ &\quad + K_{\text{a}(\text{apOH})} K_{\text{a}(\text{pyOH})} [\text{H}^+]^2 \end{aligned}$$

can be kinetically defined and eq. (6) can be derived by taking into consideration that the pro-

tonation/deprotonation processes at the donating groups of **1** and the aqua-metal ion are much faster than the coordination one.^{1,2,11} The coefficient, k_{ij} ($i = 2, 3; j = 3, 4$), is the forward rate constant for the pathway of $\text{Fe}(\text{OH})_{3-i}^{i+}$ and $\text{H}_j\text{pha}^{(j-2)+}$. Here, the rate constant of the backward reaction of Reaction (III) can reasonably be neglected because β_{11} is very large and because the relation between k_{obsd} and C_L/C_M can be extrapolated to the zero intercept with decreasing C_L .

In the same way as has been described,^{1,2} $k_{\text{obsd}'}$ can be defined and represented as given in eq. (7) on the basis of eq. (6):

$$\begin{aligned} k_{\text{obsd}'} &\equiv k_{\text{obsd}} (1 + K_{\text{OH}}^{11} / [\text{H}^+]) \alpha_{\text{H}} / C_L \\ &= k_{34} K_{\text{a}(\text{apOH})} K_{\text{a}(\text{pyOH})} K_{\text{a}(\text{amNH})} [\text{H}^+]^3 \\ &\quad + (k_{33} + k_{24} K_{\text{OH}}^{11} K_{\text{a}(\text{amNH})}) \\ &\quad \times K_{\text{a}(\text{apOH})} K_{\text{a}(\text{pyOH})} [\text{H}^+]^2 \\ &\quad + k_{23} K_{\text{OH}}^{11} K_{\text{a}(\text{pyOH})} K_{\text{a}(\text{apOH})} [\text{H}^+] \end{aligned} \quad (7)$$

The plot of $k_{\text{obsd}'}$ vs $[\text{H}^+]$ according to eq. (7) is depicted in Fig. 3. A least-squares treatment of this plotting reveals that this relation can well be approximated by a quadratic function with a zero intercept of the form shown in eq. (8).

$$Y = aX^2 + bX \quad (8)$$

Here, Y and X mean $k_{\text{obsd}'}$ and $[\text{H}^+]$, respectively, and a and b are constants including k_{ij} . This result indicates that the iron(III) complex of **1** forms through two parallel pathways of Fe^{3+} and H_3pha^+ (k_{33}) and FeOH^{2+} and $\text{H}_4\text{pha}^{2+}$ (k_{24}) and also ano-

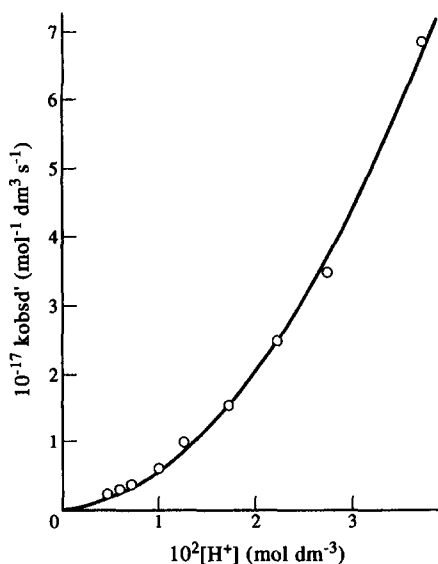


Fig. 3. Relation between $k_{\text{obsd}'}$ and $[\text{H}^+]$. $k_{\text{obsd}'} \equiv k_{\text{obsd}} (1 + K_{\text{OH}}^1 / [\text{H}^+]) (K_{\text{a}(\text{apOH})} K_{\text{a}(\text{pyOH})} K_{\text{a}(\text{amNH})} [\text{H}^+]^3 + K_{\text{a}(\text{apOH})} K_{\text{a}(\text{pyOH})} [\text{H}^+]^2) / C_{\text{L}}$. $C_{\text{L}} \gg C_{\text{M}}$; $C_{\text{L}}, 2.01 \times 10^{-3} \text{ mol dm}^{-3}$; $C_{\text{M}}, 1.00 \times 10^{-4} \text{ mol dm}^{-3}$; 0.10 mol dm^{-3} (NaClO_4), 25°C .

ther pathway of FeOH^{2+} and H_3pha^+ (k_{23}). The rate constants and their pathways thus estimated are listed in Table 3 together with those of our concern.

DISCUSSION

Formation and stability

The hypothesis of the liberations of three protons in Equilibrium (1) gave a best-fitted straight line between the absorbance and the hydrogen ion concentration terms of eq. (2). Therefore, the pyridyl nitrogen is concluded to be still protonated and non-coordinating in the iron(III) complex because of its steric hindrance, which conforms that the predominant ligand species in the acidity region for the complex formation accompanies a protonated pyridyl nitrogen (*cf* $K_{\text{a}(\text{pyNH})}$). This protonation behaviour is identical with that of Fe(III)- N^α -pyridoxyl-L-amino acid systems.^{1,2}

The stability constants of the mono(ligand) iron(III) complexes of **1** and other N^α -pyridoxyl-L-amino acid ligands listed in Table 2 indicate that the complex of **1** has a stability constant of the same magnitude as that of the tetradentate ligand, **5**, both of which are larger than the stability constants of the terdentate ligands, **2** and **3**, but smaller than the constant for **4**. This fact reflects that the affinity of the phenolato oxygen to iron(III) is larger than that of the carboxylato one and that this increased

stability by the phenolato oxygen corresponds in magnitude to the chelate effect by a methyl-carboxylato group of the tetradentate ligand. Additionally, the formation equilibrium curve of the mono(ligand)iron(III) complexes depicted in Fig. 2 clarified that the complex of **1** (Curve 1) formed in a more acidic region than the complex of **3** (Curve 2). This behaviour also supports the higher affinity of the phenolato oxygen to iron(III) than the carboxylato oxygen in the stability.

The stepwise stability constant, $\log \beta_{12} / \beta_{11}$, of the iron(III) complex of **1** is much larger than $\log \beta_{11}$, which is in contradiction to other typical iron(III)-aminocarboxylic acid systems (*cf* Table 2).¹²⁻¹⁴ This unusual tendency was also found in the iron(III)- N^α -pyridoxyl-L-amino acid systems,^{1,2} although it is less evident than that of the iron(III)-**1** system. This fact suggests that there exists an intramolecular interaction between the coordinated ligand molecules in the iron(III)-**1** stronger than those of the iron(III)-**2**, **-3** and **-4** systems. A molecular model consideration also reveals that a π - π interaction¹⁵ can be easily recognized between the pyridine ring of one ligand molecule and the benzene ring of the other in the iron(III)-**1** system (**6**) as compared with the iron(III)-**2** system (**7**) (*cf* Fig. 4).

Kinetics and mechanisms

The composite rate constant for the pathways of $\text{Fe}^{3+} + \text{H}_3\text{pha}^+$ (k_{33}) and $\text{FeOH}^{2+} + \text{H}_4\text{pha}^{2+}$ (k_{24}) is reasonable in magnitude [$(1.40 \pm 0.20) \times 10^2 \text{ mol}^{-1} \text{ dm}^3 \text{ s}^{-1}$] when compared with some reported formation kinetic results of the iron(III) complexes (*cf* Table 3).¹⁶⁻²⁰ It is of the same magnitude as the rate constants for the formation of the iron(III) complexes with N^α -pyridoxyl-L-amino acid ligands.^{1,2}

The rate constant for the pathway of $\text{FeOH}^{2+} + \text{H}_3\text{pha}^+$ [k_{23} : $(2.44 \pm 0.30) \times 10^2 \text{ mol}^{-1} \text{ dm}^3 \text{ s}^{-1}$] is almost the same as that for the complex formation reaction between FeOH^{2+} and phenol (k_{21} : $7.2 \times 10^2 \text{ mol}^{-1} \text{ dm}^3 \text{ s}^{-1}$)¹⁸ and of the corresponding pathways of iron(III)- N^α -pyridoxyl-L-amino acid systems (*cf* Table 2).

Thus, it is reasonable to deduce that the mechanistic rate-determining step is the coordination of either of two phenolato oxygens of **1** to Fe^{3+} or FeOH^{2+} . These two oxygen atoms, that are not on the aminophenol moiety but on the pyridoxyl one, may be responsible for the kinetic process, the former of which would be still protonated for its strong basicity at the rate-determining step, because all reaction pathways and their rate constants were almost identical with those of the iron(III)- N^α -pyr-

Table 3. Formation pathways and rate constants

Ligand	Pathways ^a	k_{ij} (mol ⁻¹ dm ³ s ⁻¹)	Remarks	Ref.
1 (H ₂ pha)	Fe ³⁺ + H ₃ L ⁺ (k_{33}) and FeOH ²⁺ + H ₄ L ²⁺ (k_{24})	$(1.40 \pm 0.20) \times 10^{2b}$	0.10 mol dm ⁻³ (NaClO ₄), 25°C	This work
	FeOH ²⁺ + H ₃ L ⁺ (k_{23})	$(2.44 \pm 0.30) \times 10^{2c}$	0.10 mol dm ⁻³ (NaClO ₄), 25°C	This work
2 (H ₂ plpa)	Fe ³⁺ + H ₃ L ⁺ (k_{33}) and FeOH ²⁺ + H ₄ L ²⁺ (k_{24})	$(1.08 \pm 0.20) \times 10^{2d}$	0.10 mol dm ⁻³ (NaClO ₄), 25°C	1
	FeOH ²⁺ + H ₃ L ⁺ (k_{23})	$(1.27 \pm 0.30) \times 10^{3c}$	0.10 mol dm ⁻³ (NaClO ₄), 25°C	1
3 (H ₂ plal)	Fe ³⁺ + H ₃ L ⁺ (k_{33}) and FeOH ²⁺ + H ₄ L ²⁺ (k_{24})	$(1.08 \pm 0.20) \times 10^{2d}$	0.10 mol dm ⁻³ (NaClO ₄), 25°C	1
	FeOH ²⁺ + H ₃ L ⁺ (k_{23})	$(5.25 \pm 0.30) \times 10^{3c}$	0.10 mol dm ⁻³ (NaClO ₄), 25°C	1
4 (H ₂ pltp)	Fe ³⁺ + H ₃ L ⁺ (k_{33}) and FeOH ²⁺ + H ₄ L ²⁺ (k_{24})	$(4.40 \pm 0.20) \times 10^{2d}$	0.10 mol dm ⁻³ (NaClO ₄), 25°C	2
	FeOH ²⁺ + H ₃ L ⁺ (k_{23})	$(9.94 \pm 0.30) \times 10^{2c}$	0.10 mol dm ⁻³ (NaClO ₄), 25°C	2
5 (H ₃ plpas)	Fe ³⁺ + H ₃ L (k_{33}) and FeOH ²⁺ + H ₄ L ⁺ (k_{24})	$(5.22 \pm 0.20) \times 10^{1e}$	0.10 mol dm ⁻³ (NaClO ₄), 25°C	1
	FeOH ²⁺ + H ₃ L (k_{23})	$(1.31 \pm 0.30) \times 10^{2c}$	0.10 mol dm ⁻³ (NaClO ₄), 25°C	1
Hpdx-L-Htrp	Fe ³⁺ + H ₂ pdx-L-Htrp ⁺ (k_{33})	$k_{33}: 10.1 \pm 0.30$	0.50 mol dm ⁻³ (NaCl), 25°C	16
	FeOH ²⁺ + H ₂ pdx-L-trp (k_{22})	$k_{22}: 32.5 \pm 0.30$	0.50 mol dm ⁻³ (NaCl), 25°C	16
ClCH ₂ COOH	FeOH ²⁺ + ClCH ₂ COOH (k_{21})	$k_{21}: (8.30 \pm 0.20) \times 10^3$	0.10 mol dm ⁻³ (NaClO ₄), 25°C	17
		$k_{21}: (6.8 \pm 0.1) \times 10^3$	0.10 mol dm ⁻³ (NaClO ₄), 25°C	18
C ₆ H ₅ OH	Fe ³⁺ + C ₆ H ₅ OH (k_{31})	$k_{31}: \sim 25$	0.10 mol dm ⁻³ (KNO ₃), 25°C	18
	FeOH ²⁺ + C ₆ H ₅ OH (k_{21})	$k_{21}: 7.2 \times 10^2$	0.10 mol dm ⁻³ (KNO ₃), 25°C	19
C ₆ H ₅ OH	FeOH ²⁺ + C ₆ H ₅ OH (k_{21})	$k_{21}: 1.1 \times 10^3$	0.10 mol dm ⁻³ (NaClO ₄), 25°C	19
		$k_{21}: 1.5 \times 10^3$	0.10 mol dm ⁻³ (NaClO ₄), 25°C	20

^aL denotes the fully-deprotonated ligand species of the ligands **1–5**.

^b $k_{33} + k_{24}K_{OH}^{11}Ka_{(amNH)}$.

^c k_{23} .

^d $k_{33} + k_{24}K_{OH}^{11}Ka_{(COOH)}$.

^e $k_{33} + k_{24}K_{OH}^{11}Ka_{(mcCOOH)}$.

idoxyl-L-amino acid systems (cf Table 3).^{1,2} Therefore, it can be concluded that the ligand **1** adopts the following general kinetic characteristics of the iron(III)-*N*^α-pyridoxyl-L-amino acid systems;^{1,2} the rate-determining coordination of the phenolato oxygen of the pyridoxyl moiety to iron(III), fol-

lowed by the rapid donations of the amino nitrogen and another phenolato oxygen to form six- and five-membered fused chelate rings in the iron(III)–**1** system as depicted in Scheme 1.

In summary, the ligand **1** forms a very stable bis(ligand)iron(III) complex. The existence of a

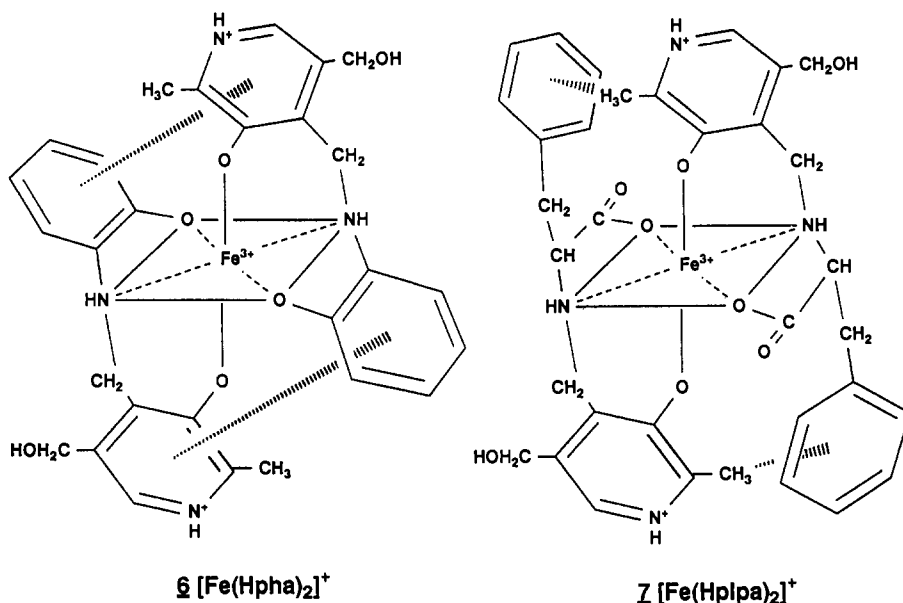
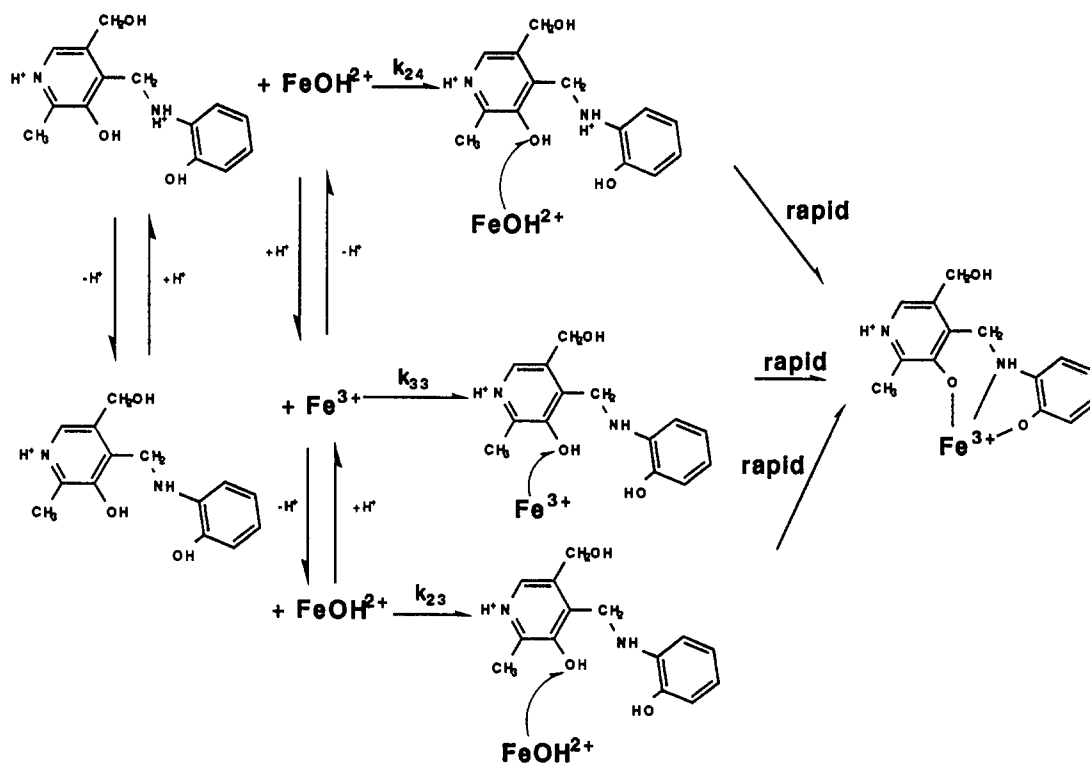


Fig. 4. The estimated structures of the bis(ligand)iron(III) complexes of **1** and related ligand **2**.



strong π - π intramolecular interaction, which is evidenced from the stepwise stability constants, in the bis(ligand)iron(III) complex of **1** suggests us to design an artificial siderophore having a pyridoxal moiety by introducing another moiety capable of

forming an intramolecular interaction for the enhancement of the thermodynamic stability in the metal complex. Specifically, *o*-aminophenol group can be recommended as one of the best partner moiety of this type of ligand.

REFERENCES

1. T. Ozawa, K. Jitsukawa, H. Masuda and H. Einaga, *Ber. Buns. Phys. Chem.* 1994, **98**, 66.
2. T. Ozawa, K. Jitsukawa and H. Einaga, *Ber. Buns. Phys. Chem.* 1994, **98**, 59.
3. L. D. Loomis and K. N. Raymond, *Inorg. Chem.* 1992, **30**, 906.
4. M. Noritake, K. Okamoto, J. Hidaka and H. Einaga, *Bull. Chem. Soc. Jpn.* 1990, **63**, 353.
5. J. Kielland, *J. Am. Chem. Soc.* 1937, **59**, 1675.
6. Y. Hara, K. Okamoto, J. Hidaka and H. Einaga, *Bull. Chem. Soc. Jpn.* 1984, **57**, 1211.
7. R. M. Smith and A. E. Martell, *Critical Stability Constants*, Vol. 2, p. 8. Plenum, New York (1975).
8. Ref. 7, p. 72.
9. L. G. Sillén and A. E. Martell, *Stability Constants of Metal-Ion Complexes*, Special Publication No. 17, p. 53. Chemical Society, London (1964).
10. R. M. Smith and A. E. Martell, *Critical Stability Constants*, Vol. 6, p. 98. Plenum, New York (1974).
11. M. Noritake, K. Jitsukawa and H. Einaga, *Ber. Buns. Phys. Chem.* 1992, **96**, 857.
12. Ref. 10, p. 2.
13. Ref. 10, p. 38.
14. Ref. 10, p. 68.
15. For example: O. Yamauchi, A. Odani, T. Kohzuma, H. Masuda, K. Toriumi and K. Saito, *Inorg. Chem.* 1989, **28**, 4066.
16. H. Kuno, K. Okamoto, J. Hidaka and H. Einaga, *Bull. Chem. Soc. Jpn.* 1989, **62**, 2824.
17. B. Perlmutter-Hayman and E. Tapuhi, *J. Coord. Chem.* 1976, **6**, 31.
18. S. Gouder and J. Stuehr, *Inorg. Chem.* 1974, **13**, 379.
19. K. Nakamura, T. Tsuchida, A. Yamagishi and M. Fujimoto, *Bull. Chem. Soc. Jpn.* 1973, **46**, 456.
20. F. P. Cavalasino and E. D. Dio, *J. Chem. Soc. A* 1970, 1151.